https://link.springer.com/article/10.1007/s10518-018-0333-9

AUTHOR'S POST-PRINT VERSION

VIEW-ONLY PUBLISHER VERSION AVAILABLE HERE

DOWEL CONNECTIONS SECURING ROOF-DIAPHRAGMS TO PERIMETER WALLS IN HISTORIC MASONRY BUILDINGS AND IN-FIELD TESTING FOR CAPACITY ASSESSMENT

Alessandra Marini[1], Ezio Giuriani[2], Andrea Belleri[3], Stefania Cominelli[4]

[1] Associate Professor, University of Bergamo, Italy; alessandra.marini@unibg.it

[2] Full Professor, University of Brescia, Italy; ezio.giuriani@unibs.it

[3] Assistant Professor, University of Bergamo, Italy; andrea.belleri@unibg.it

[4] Post Doc, University of Brescia, Italy; stefania.cominelli@unibs.it

Abstract

In the seismic retrofit of existing masonry constructions, global interventions are often needed to inhibit the onset of local mechanisms and to engage the whole building box-like structural behaviour. Such interventions are represented by perimeter ties and roof and floor diaphragms. This paper considers the roof diaphragm strengthening solution and investigates the use of stud connections securing the roof thin-folded shell to the perimeter walls. Stud connections serve the dual purpose of collecting and transferring the out-of-plane inertia forces of the masonry walls to the roof diaphragm, as well as transferring the diaphragm reaction forces to the shear walls. Specific detailing of the stud connection and the adoption of an improved lime-mortar overlay on the top of the masonry walls are proposed to improve the connection strength; without such improvements, the connection capacity would be jeopardised by the reduced shear resistance of the masonry wall due to the absence of significant vertical confining action at the roof level. The intervention entirely changes the behaviour of the connection and significantly reduces shear stresses on the masonry wall.

The structural behaviour of the connection is analysed and discussed. Emphasis is made on the conceptual design of laboratory and in-field test procedures and testing frames in order to replicate the boundary conditions in real applications. In-situ tests may help during the design of the roof thin-folded shell system and allow for the efficiency assessment of the connections prior to the final intervention, thereby proving the actual feasibility of the retrofit solution.

Keywords

Historic masonry buildings, seismic retrofit, roof diaphragm, roof thin folded shell, stud connection, stud capacity in masonry walls, field testing.

1. INTRODUCTION AND RESEARCH SIGNIFICANCE

The remarkable damage surveyed on historical buildings in the aftermath of recent earthquakes is mainly due to either the poor quality of the masonry walls, or to a lack of conceptual design with respect to horizontal actions, or both. When the quality of the masonry is poor, or when the masonry walls are arranged as two- or three-leaf walls devoid of any interlocking of the leaves, the building may crumble in the event of an earthquake, without the onset of the typical local failure mechanisms involving macro-elements of the buildings. On the other hand, when the quality of the masonry is not an issue, the seismic vulnerability of existing buildings is often caused by the absence of a seismic-resistant structural system or by its poor conceptual design, resulting in the inability of the structure to retain the perimeter walls under out-of-plane seismic loads (Turnšek et al. 1978, D'Ayala and Speranza 2002, Giuriani and Marini 2008a). In the latter case, despite the good quality of the masonry, damage can be so severe as to lead to the total or partial collapse of the building. Wooden floors, vaults and existing timber roofs are unable to inhibit the out-of-plane wall detachment and, in the worst scenario, the wall overturning (Fig. 1). Considering churches, additional damage and collapse of the vaults could be triggered by the rocking motion of the diaphragm arches (Lagomarsino et al. 2004, Giuriani et al. 2009, Ferrario et al. 2009, Fig.2). Examples of all these typical failures have been repeatedly observed after the recent earthquakes in Central Italy (2016), as for instance in the church of Sant'Agostino in Amatrice, where the major damage was caused by the onset of the overturning of the façade and the lateral walls (Fig.1a), or in Sant'Emidio church, housing the civic museum in Amatrice, where severe rocking of the nave arches was observed (Fig. 2c).

a)   b)

Figure 1. Typical failure mechanism involving the overturning of the perimeter walls: a) Overturning of the façade and lateral walls in S. Agostino Church (as it was after the first shock of August 2016); b) detachment of a perimeter wall in Villa Galvagnina hit by the Emilia earthquake in 2012.
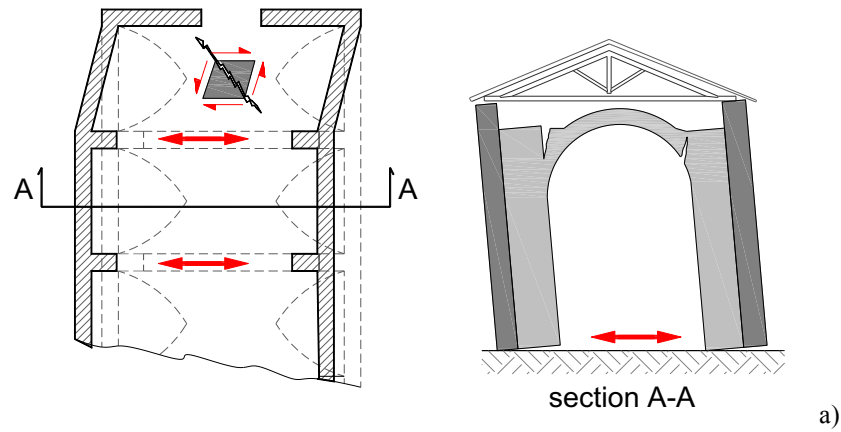
Figure 2. Possible failure mechanisms: a) rocking and differential rocking of transverse arches; b) collapse of the vault induced by direct and indirect bending; c) rocking of the nave arches in S. Emidio Church in Amatrice.

The priority mitigation measures aimed at reducing these vulnerabilities consist of the preliminary improvement of the quality of the masonry, if necessary, and the adoption of either perimeter ties or floor and roof diaphragms, inhibiting the onset of partial or global overturning of the perimeter

walls (Tomăzevič 1989, Eurocode 8, Giuriani and Marini 2008, Modena et al. 2009, D'Ayala 2014, among others).

It is worth noting that in the case of elongated buildings with large openings and devoid of floors, such as churches and theatres, the perimeter ties are generally unable to effectively constrain the perimeter walls due to the high slenderness of the wall, even if the quality of the masonry is good. In such conditions the arch-tie mechanism is ineffective (Fig.3) and roof diaphragms are necessary to bind the perimeter walls and avoid overturning (Fig.4), thereby enabling a box-like behaviour. Roof diaphragms (also referred to as roof shell structure below) were first proposed as a retrofit measure in historical buildings following the Salò earthquake (Italy, 2008) (Marini and Giuriani 2006, Giuriani and Marini 2008b), and later adopted to enhance the seismic performance of several churches damaged in the Emilia earthquake (Italy, 2012).
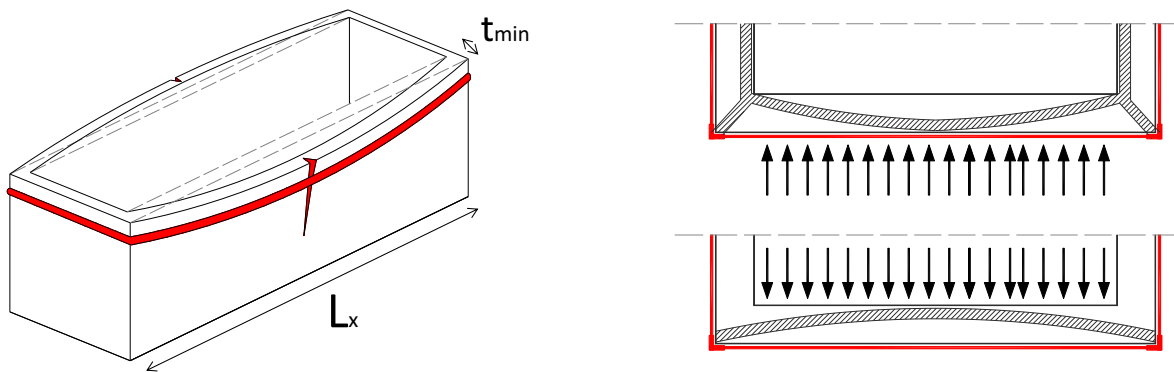

Figure 3. Perimeter ties may be ineffective in the case of oblong buildings because of the remarkable slenderness of the perimeter walls, which may result in a poor tied-arch mechanism.

Figure 4. a) Schematic and b) aerial view of a roof shell structure, c) stud connections securing the roof shell structure to the perimeter walls.

The static behaviour of roof diaphragms is conceived by considering the structure as formed by folded pitch plates (Fig.5, Marini and Giuriani 2006, Giuriani and Marini 2008b, Giuriani et al. 2016, Preti et al. 2017). The roof diaphragm collects the inertia forces of the roof and the out-of-plane loaded masonry walls and transfers them to the seismic resistant walls. The roof shell

structure is composed of perimeter chords that resist the shell bending action and of web panels that resist shear actions. The roof shell is usually made of wooden panels, a double wooden plank overlay, or light metal trusses, whereas perimeter chords are made of steel plates. These lightweight solutions are also suitable for historic buildings as they can be assembled over the existing wooden roof structures, and are respectful of the strict preservation requirements that characterise such buildings (Hume 1991, Carbonara 2003, among others); the solution is fully compatible with the existing building both from an architectural and seismic point of view, as it provides a negligible change in the building's shape and volume, with a limited increase of the seismic mass.

The solution also applies to the strengthening of churches featuring transverse arches and vaults. In such cases the roof diaphragms provide a constraint on the extrados of the transverse-arches that inhibits the possible failure mechanisms following the unconstrained rocking of the piers or the differential rocking of the nave bays, thereby protecting the nave vaults.

The use of a roof shell structure may also reduce the seismic vulnerability of some ordinary buildings, especially when the upper portion of the wall above the top floor diaphragm is exposed to the risk of overturning due to the lack of constraint at the roof level.

The role of the connections to the load-bearing walls is fundamental in the conceptual design of the roof shell structure. The same applies for the connections to transverse arches in churches. These connections are usually made by means of steel dowels or studs (Fig. 5 and 6), which fulfil the strict compatibility requirements of historic monument preservation as they are not invasive and mostly reversible. Dowels are made from round smooth steel rods and driven into vertical cylindrical holes created in the masonry by means of core drills. The role of the dowel connections depends on the location along the top of the masonry walls: they retain the walls subjected to out-of-plane inertia loads and transfer the seismic action to the roof diaphragm (Fig. 5 and 6, type b); they secure the upper portion of the masonry walls of possible transverse-arches to the roof diaphragm (Fig. 5 and 6, type c); finally, they transfer the seismic load collected by the diaphragm to the seismic-resistant shear walls (Fig. 5 and 6, type a). The stud behaviour is usually assumed as rigid, provided that the sliding deformation of the connected parts is negligible.

Finally, additional connections made by means of grouted deep anchors are placed along the top of the masonry walls to prevent roof uplift; such connections also establish an effective bond between the restored upper courses of the masonry walls and the underlying portions (d in Fig. 6, Giuriani and Marini 2008b).
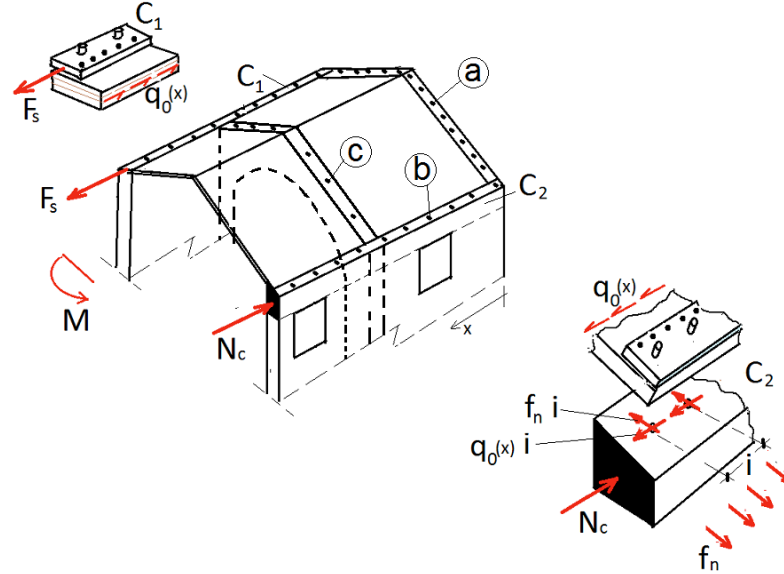
Figure 5. Reference static scheme for the evaluation of the internal action in each roof shell structure component.
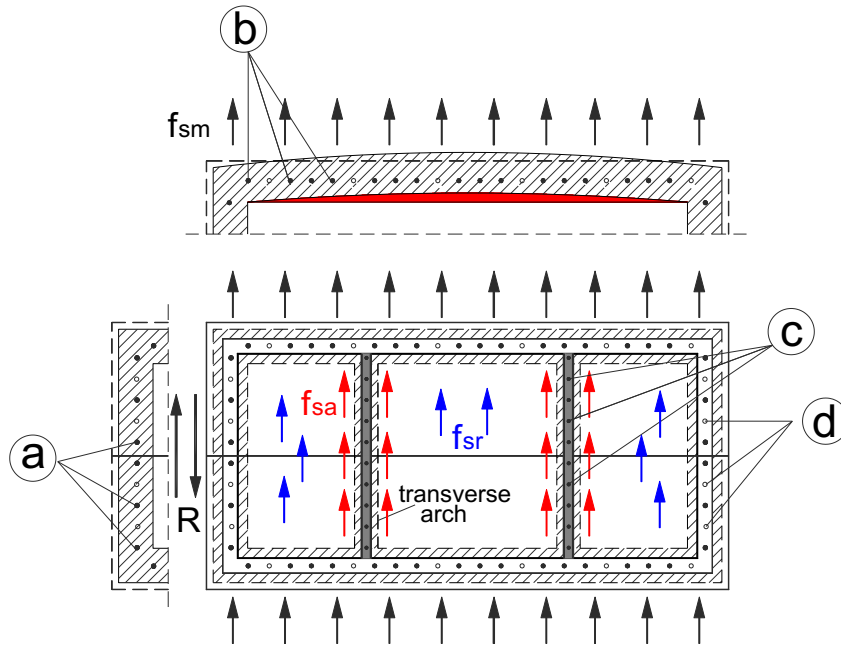

Figure 6. Planar view of a roof shell structure with emphasis on the different types of connections required to secure the roof diaphragms to the perimeter walls: studs transferring shear actions to the shear walls (type a); studs collecting and transferring the inertia forces of both the longitudinal walls (type b) and the transverse arches (type c) to the roof shell structures; and deep anchorages preventing possible roof uplift (type d).

The use of steel dowels to transfer the shear forces between two structural parts is not new. The first scientific studies and applications focused on the connections between RC slabs and steel beams in bridges with a composite cross-section (Mainstone and Menzies 1967, Menzies 1971, Oehlers and Johnson 1987, Shim 2004, Johnson 2008, among others). Dowels are also adopted as metal fasteners between glulam timber elements (Eurocode 5), in the precast industry and in the retrofit of existing wooden floors. In the latter case, they enable the composite behaviour of the existing joists

7

and the additional extrados reinforcing elements, such as steel beams, thin plates or light concrete overlays (Piazza and Turrini 1983, Ronca et al. 1991, Ahmadi and Saka 1993).

In the past, the analytical formulation of the dowel connection stiffness has been derived by considering the stud as a beam on elastic supports (Gelfi et al., 2002, Xue et al. 2008, Auclair et al. 2016, among others); experimental results substantiated the accuracy of the model when the dowel is surrounded by continuum materials such as concrete or wood. As for the ultimate strength of the connection, specific theoretical studies (Johnson and Oehlers 1996, among others), as well as experimental tests on steel-concrete composite sections (Stark and van Hove in 1991, among others), have shown the reliability of modeling the connection failure as triggered by the development of two plastic hinges along the stud shank. Specific studies on the stress distribution along the loaded area (Biolzi and Giuriani 1990) showed that the concrete matrix exhibits almost perfect elasto-plastic behaviour upon overcoming the load bearing strength. Theoretical predictions of the dowel capacity are in good agreement with the experimental results (Gattesco and Giuriani 1996, Zandonini and Bursi 2002, Pallarés and Hajjar 2010, among others) and with some empirical (Eurocode 5) and analytical formulations available in the literature (Gelfi et al., 2002, Auclair et al. 2016, among others).

To the authors' knowledge, the use of dowel connections in historic buildings to enable shear load transfer between structural elements and masonry walls was only proposed and scientifically investigated in recent years (Giuriani and Marini and 2008b, Giuriani 2011). Unlike steel-to-concrete, wood-to-concrete and wood-to-wood connections, in the case of historical masonry walls the available formulations may lose validity due to the high local heterogeneity of the masonry (Cominelli et al. 2017). In the case of stone masonry walls, the behaviour of the dowel depends on the size and shape of the stone blocks and, most importantly, on its location with respect to the stone, i.e. in the central part of the stone or in proximity to the mortar joint. For small stone elements, the resisting mechanism is governed by the possible displacement of the stone (Giuriani et al. 1993, Felicetti et al. 1997, Gattesco and Del Piccolo 1998); while the behaviour of the dowel may differ if placed in a larger diameter hole filled with resin or mortar (Giuriani 2011). In the case of brick masonry walls, the bearing capacity depends on the dowel position with respect to the mortar joints (Giuriani 2011). Therefore, the different local characteristics of the material that surrounds the dowel as well as the connection layout should be considered in the structural modelling of connections. The complexity and heterogeneity of the masonry make it unfeasible to use global three-dimensional numerical modelling; such an approach would require sound knowledge and effective modelling of local complex interactions between mortar and stone

elements, or between mortar and bricks, as well as the constitutive laws of the mortar under a three-dimensional stress state.

Given the above, this paper proposes a minimally impairing technical solution for the connection between roof diaphragms and the underlying masonry walls, introducing a thin mortar slab to improve the connection capacity. The thin overlay is required due to the inability of the masonry at the top of the walls to withstand shear point loads in the absence of vertical confinement. When appropriately designed, the intervention substantially changes the behaviour of the connection and dramatically reduces the stresses at the top of the masonry wall; the connection capacity becomes less sensitive to the heterogeneous properties of the masonry but it rather depends on the properties of the thin, high-performance lime mortar slab. A special test setup and procedure, suitable for both laboratory and on-site testing, is proposed to assess the efficiency of the connections; the test setup allows the actual boundary conditions of the roof shell structures to be accounted for. An analytical formulation is presented to provide a preliminary estimate of the strength of the connection; such formulation is useful for design professionals in the initial proportioning of the connection. It is worth noting that the model can be adopted only if the thin, high-performance slab is introduced, i.e. the connection capacity is governed by the strength of the mortar layer. Nonetheless, in-field tests are mandatory to assess correct execution of the connections, and the achievement of effective performances of the thin lime mortar slab. Finally, some relevant experimental results are presented in the paper. The tests allow for the comparison between the predicted and observed behaviour of the dowel connection and provide useful reference values.

2. TECHNOLOGICAL ISSUES AND STRUCTURAL BEHAVIOUR OF DOWELS

Dowels are typically obtained from smooth galvanised steel rods (Fig. 7) and they are dry-driven into tight-fitting holes which are core-drilled into the top of the masonry wall, or placed into larger holes subsequently injected with either epoxy resins or, more frequently, with compatible lime-based mortars. The shear strength of the dowel depends on the steel grade, particularly on the yield stress of the steel, and on the local characteristics of the masonry. When the length of the dowel enables activation of the so called "long-dowel" behaviour (Gelfi et al. 2002), dowel failure follows the onset of two plastic hinges along the stud shank. The location of the plastic hinges determines the effective length of the dowel (the length along which the shear action is actually transferred), and in turn the ultimate strength of the dowel. The location of the plastic hinges depends on the local deformation of the material surrounding the stud shank, and it is usually calculated by assuming a distribution of uniform bearing stresses along the embedment lengths of the stud shank.

In the case of the roof shell structures considered herein, the proposal of an analytical model that accurately predicts the behaviour of the roof-to-wall connection is almost unviable due to the substantial local heterogeneity of the masonry. Analytical formulations for roof-to-wall dowel connections are only reliable if connectors are embedded into pre-consolidated masonry walls, from which a significant improvement of the local behaviour of the masonry is obtained.

In this paper, pre-consolidation of the top of the masonry walls to increase the capacity of the connection is proposed. Pre-consolidation can be obtained by rearranging the top courses of the masonry by repositioning or replacing any loose stones and bricks and by using good quality mortars, and by introducing a thin structural lime mortar layer on top of the masonry walls (Fig. 7a and 8). Indeed, when the thickness of the mortar layer is greater than the effective length of the dowel (Gelfi et al. 2002), the connection can be assumed as a dowel completely embedded into a homogeneous material and the maximum capacity of the dowel is exploited, as explained in the next section. In this scenario, the improved lime mortar overlay allows the shear loads to be spread as tangential stresses along the interface with the underlying masonry walls as highlighted in the next section. The absence or inefficiency of such mechanism will lead to concentrated loads in the dowels beneath the mortar layer, with point shear loads in the masonry causing its possible early failure.

For the overlay, premixed high-performance lime mortars with 15÷18MPa compressive strength are recommended. The structural overlay is strengthened with a few layers of glass fibre mesh (with a tensile resistance ranging between 50÷100 kN/m), or with welded mesh made of galvanised steel wires. Interestingly, this pre-consolidation technique introduces a layer of nearly homogeneous material that may plastically deform when subjected to the dowel action.

The effective length of the dowel develops in such a mortar layer when the layer thickness is higher than 4÷5 cm; indeed, the effective length is typically 1.5÷2 times the dowel diameter, as obtained from the analytical formulation presented in the next section. If the thickness of the mortar layer is lower than the effective length of the dowel, the analytical formulations are unsuitable and unreliable, and the load-bearing capacity of the stud connection can only be directly assessed through in-field tests. It is worth noting that, including in the case of pre-consolidated masonries, experimental tests should always be aimed towards assessing correct execution of the intervention, and thus towards validating the theoretical prediction of the connection capacity.

It is essential to note that the use of the proposed lime mortar overlay is only intended to improve the capacity of the connections, whereas it is not intended as a retrofit of the masonry wall underneath. Retrofit of the masonry walls is mandatory prior to any other strengthening measure in

10

the case of poor or very poor quality masonry, as may occur in historical constructions. For example, when the upper floor masonry walls are made of either three or two leaves lacking an effective interlocking of the withies, preliminary retrofit of the masonry must be carried out. An example of such a retrofit is shown in Figure 7b, where the "monolithic" behaviour of the masonry is enforced through the adoption of artificial bonders, such as transverse ties and structural plaster, and with the filling of the cavities with lime mortar injections (Fig. 7b). Discussion of such retrofit, however, lies beyond the scope of this paper.

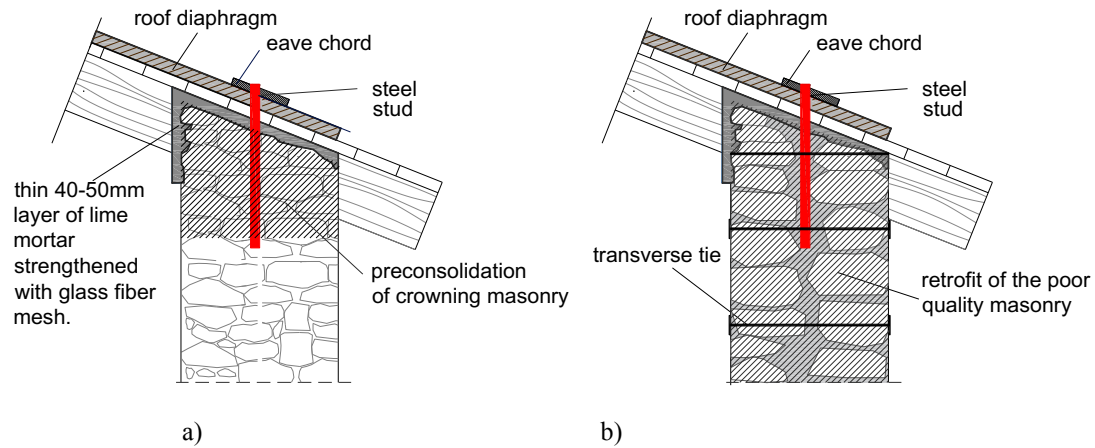a)   b)

Figure 7. a) Masonry pre-consolidation obtained from rearranging the top courses of the masonry wall by repositioning or replacing loose stones and bricks, by adopting good quality mortars and by introducing a structurally improved lime mortar overlay on top of the masonry walls; b) in the case of two- or three-leaf walls lacking the bonders, substantial retrofit must be preliminarily carried out, including transverse ties, local injection and structural plaster, if necessary, to improve the interlocking of the leaves.

Figure 8. View of the thick lime mortar layer, pre-consolidating the top portion of the peripheral walls.

3. ESTIMATING THE DOWEL CAPACITY

When the mechanical characteristics of the masonry are very good or in the case of preliminary pre-consolidation of the top of the masonry walls, the failure mechanism of the roof-to-masonry connections resembles that of the connectors in composite beams, and it is mostly a function of both the dowel length and the bearing strength of the materials (Gelfi et al. 2002, Giuriani and Grisanti 1986). With reference to roof-to-masonry connections, the dowel capacity is a function of the dowel

diameter, the yield strength of the steel, the bearing strength of the material surrounding the dowel (either the pre-consolidated masonry, the improved lime mortar layer or the good quality masonry), and the possible detachment between the metal eave chord of the roof diaphragm and the top end of the wall.

According to Gelfi et al. (2002), the dowel capacity entirely depends on the bearing strength developed along the segment A_1B (Fig.9), corresponding to the dowel effective length l_{ef}, and it is independent of the bearing stresses distributed along the segment BC. As highlighted in the previous chapter, evaluation of the bearing strength of the masonry is a difficult task because the material surrounding the dowel is highly heterogeneous, and made of either stones or bricks and lime mortar. In the case of pre-consolidation of the top of the masonry wall with the proposed structural overlay made of improved lime mortar (Fig. 7b, Fig. 8), and in the case of dowels with small diameters ϕ (ϕ < 20mm), the dowel effective length l_{ef} (Fig. 9a) is usually smaller than the thickness of the mortar layer t_m, therefore the capacity is governed by the bearing strength of the homogeneous mortar layer (f_{mh}). Under these conditions, the capacity is given by:

$$V_u = f_{mh} \varnothing l_{ef} \qquad \qquad 1)$$

where f_{mh} is the bearing strength of the dowel in the improved lime mortar layer. In detail:

$$l_{ef} = \varnothing \left[\sqrt{\left(\frac{a}{\varnothing}\right)^2 + \frac{\chi}{3}\frac{f_y}{f_{mh}}} - \frac{a}{\phi} \right] \qquad \qquad 2)$$

where: a is the distance between the steel plate p and the underlying mortar layer (Fig. 9a), usually corresponding to the thickness of the plywood web panel of the roof diaphragm; f_y is the dowel yield stress; $f_{mh}=\alpha f_m$ is the bearing strength; f_m is the compressive strength of the mortar, experimentally measured on cylindrical specimens; α=3÷3.5 is a coefficient accounting for the improved local behaviour of the mortar, which benefits from the confinement due to the three-dimensional compressive stress state developing in the proximity of the dowel (Biolzi and Giuriani 1990, Marini et al. 2018). The coefficient χ depends on the type of connection between the dowel and the steel plate (Fig. 9c and d). In the case of tight-fitting holes in the steel plate, or when the dowel is fully welded to the plate (Fig. 9c), the dowel head is prevented from rotating and χ is equal to 2. In the case of hole-stud clearances or anytime it is not welded, the dowel head can rotate (Fig. 9d) and χ is equal to 1.

Depending on the type of connector, the load demand F on the dowel (Fig. 9a) can be directly estimated. With reference to Figure 6: $F=q\,i$ for type "a" dowels, where q is the shear flow

transferred from the roof diaphragm to the walls (Giuriani and Marini 2008b) and i is the dowel spacing (Fig. 5b and 6); $F=f_{sm}\, i\, h_i$ for type "b" dowels, where f_{sm} is the seismic action per unit area of the masonry wall, and h_i is the inter-storey height; and $F=f_{sa}\, i$ for type "c" dowels, where f_{sa} is the seismic action per unit length transferred to the roof diaphragms by any transverse arches.
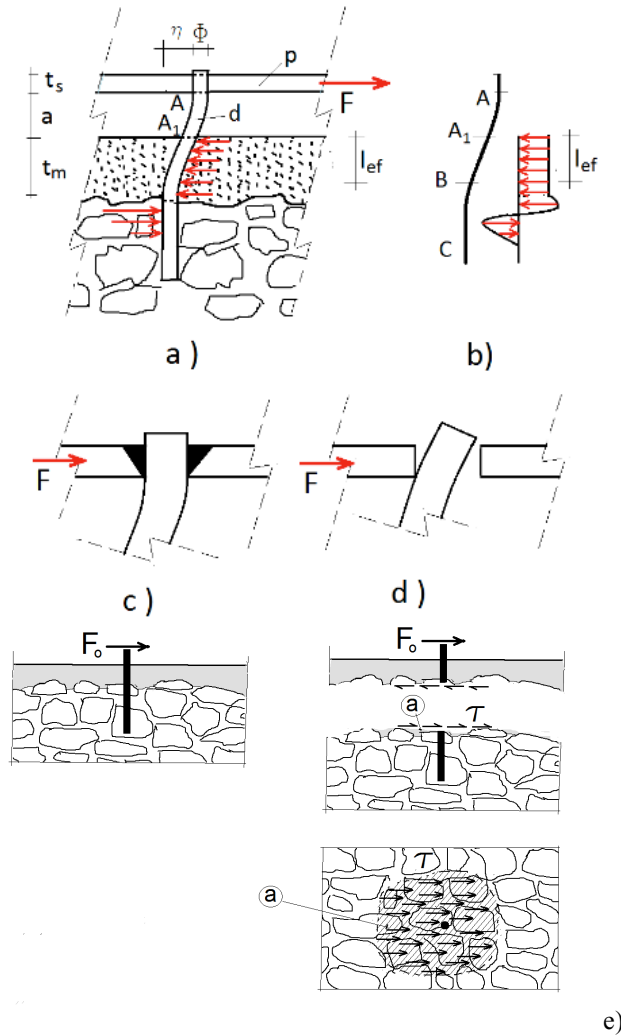
Figure 9. a) Behaviour of the stud connection securing the roof diaphragm to the pre-consolidated top of the masonry walls; b) simplified static scheme of the dowel in ultimate condition, showing the bearing strength stress distribution along the stud shank; c) stud fix end restraint offered by the steel eave chord in the case of tight-fitting holes, or when the dowel is fully welded to the plate; d) hinge restraint in the case of hole-stud clearances or when there is no welding; e) role of the improved lime mortar overlay, spreading the point load transferred by the stud into a shear stress distribution over the interface between the overlay and the masonry wall below.

It is worth remembering that the interposition of the proposed thin layer of strengthened lime mortar enhances the performance of the masonry in the areas where the stresses transferred by the dowels are higher. The load transferred by the dowel to the strengthened lime mortar layer spreads across the depth of the mortar overlay and is transferred to the masonry top courses as a shear stress distribution of significantly lower magnitude, and distributed across the area *(a)* as shown in Figure

13

9e. This solution allows the exploitation of the maximum capacity of the dowel connection, i.e. the development of the 2-hinge mechanism in the stud shank. It is worth noting that continuity of the slab can be beneficial but it is not strictly necessary, provided that the resisting mechanism, illustrated in Fig. 9e, only involves the interface between the mortar slab and the masonry walls, in proximity to the stud shank.

When no strengthening or pre-consolidation of the top of the masonry walls is envisioned, the early failure of the masonry may be triggered by either the crushing of the masonry under the high stresses transferred by the dowel, or the sliding shear failure along the upper bed joints.

4. TEST SETUP FOR LABORATORY AND IN-FIELD TESTS AND EXPERIMENTAL RESULTS

The main aim of the paper is to introduce an in-field test suitable for the assessment of the connection capacity. Such a test is required to both verify the feasibility of the roof diaphragm strengthening technique and to assess the correct on-site execution of the structural details. In this chapter, some relevant results of cyclic load laboratory and in-field tests are presented. These results are part of a comprehensive experimental campaign (Marini et al. 2016) and represent a preliminary reference for the design of dowel connections. Tests results also enable validation of the analytical formulation of the connection capacity presented in the previous section (Eq. 1).

1.1 Laboratory tests

A masonry specimen, 3.4x0.5x1 m, with 12 brick courses was built in the laboratory (Specimen A in the following). Regular 55x120x250 mm solid bricks together with a poor quality lime mortar were adopted to reproduce historical masonry properties, with a compressive strength ranging between 3÷4MPa. A thin 50 mm lime mortar overlay was cast on the top edge of the sample to replicate the strengthening of the top of the masonry wall. The overlay was made of a premixed mortar of improved characteristics, with a compressive strength of about 10 MPa after 28 days curing, 15 MPa after 120 days, and an elastic modulus of 15000 MPa. The overlay was strengthened by means of a 10x10 mm glass fibre mesh, with a tensile resistance of 30 kN/m; such a detail improved the bearing strength of the lime mortars, which rose to 44 MPa.

Studs made of 355 steel, with 20 mm diameter, were dry-driven into calibrated holes drilled across the overlay and through the masonry top edge. The stud embedment length in the masonry was approximately 400 mm. The stud spacing along the crown was 500 mm.
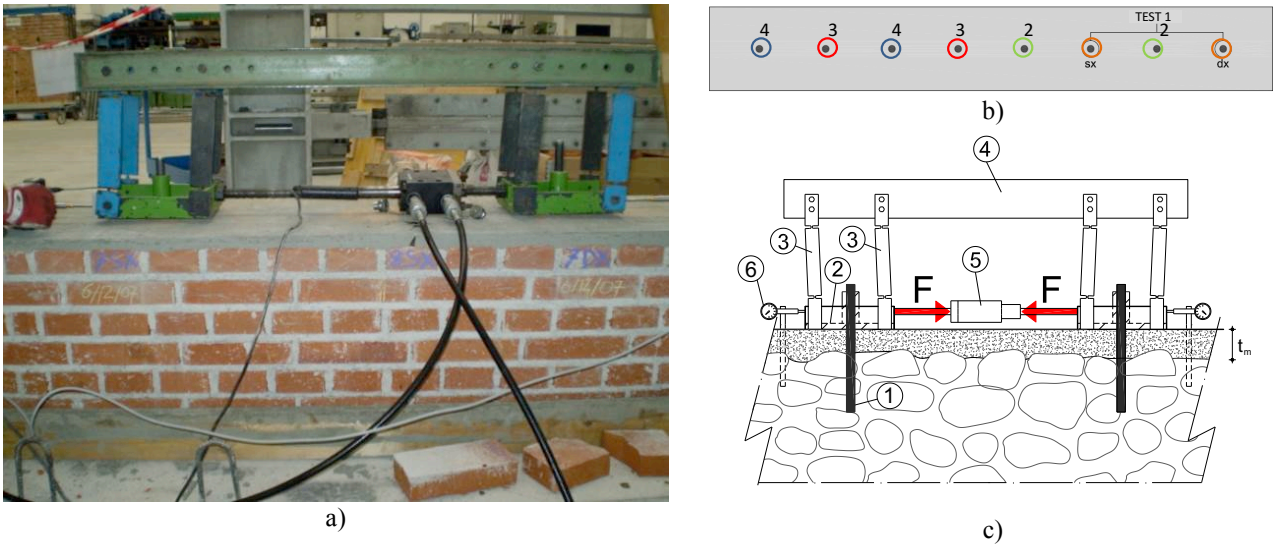
Figure 10. a) Masonry specimen and laboratory testing frame, b) pairs of studs tested in each individual test and c) schematic view of the test set up.

Laboratory testing frame and test results

Cyclic shear tests were carried out on Specimen A by adopting a special testing frame, referred to as Laboratory Testing Frame (LTF) hereinafter. The LTF was conceived in order to replicate the actual load and boundary conditions of the stud connection securing the roof shell structure to the masonry walls in real applications, in which each stud collects the tributary shear flow along the roof perimeter chords and transfers it to the masonry walls.

The testing frame illustrated in Figure 10a was used for the experimental tests. The testing apparatus is made of a metal frame connected to the dowels by means of two horizontal steel plates; the plates are interconnected through a double-acting hydraulic jack enabling the application of cyclic loads. The system allows testing of two connections at a time, for a total of 4 tests (pairs 1 to 4 in Fig. 10b).

The testing frame layout is conceived to only enable the shear action transferred through the dowels; the plates connecting the dowels are forced to slide horizontally without rotating, thereby avoiding onset of friction between the wall and the plate. For that reason, a small vertical tolerance (> 1 mm) was always provided between the horizontal plates and the wall top edge. The bending moment arising from the load eccentricity with respect to the sliding surface is counteracted by the axial actions triggered in the vertical links (*3* in Fig.10c).

In particular, the testing frame is connected to the top end of the two dowels (*1* in Fig.10c), which are driven into squat circular steel pipes welded to the horizontal plates (*2* in Fig.10c). Such an

15

assemblage specifically enables easy disassembly of the test setup and inhibits or limits the rotation of the dowel head. The horizontal plates (*2* in Fig.10c) cannot rotate due to the restraint provided by the vertical trusses (*3* in Fig.10c) connected to the transversal beam (*4* in Fig.10b). The vertical trusses are obtained from steel plates in which a double-notch reduces the cross section at the heads; such a detail ensures that only axial forces and no shear actions are transferred across the vertical link system, provided that the bending stiffness of the vertical trusses is smaller by about two orders of magnitude with respect to the bending stiffness of the dowel. Mechanical displacement transducers (*6* in Fig.10c) monitor the relative displacements between the sliding plates and the undisturbed part of the wall.

The LTF allows for an accurate study of the behaviour of the dowels under reverse cyclic loading of increasing magnitude up to the failure of the "weaker stud", with the companion stud never reaching collapse; the resulting shear-displacement curves can be compared in terms of stiffness, whereas the capacity is determined by the failure of the "weaker stud".

In the experimental test, load cycles equal to multiple of ±7.5 kN were applied to the connections up to failure. Figure 11 shows the typical load-displacement curve obtained from the tests on the stud connections for the first pairs of studs in Specimen A (Fig.10b). The initial low stiffness branch of the curves is associated with the recovery of the clearances between the stud and the vertical connecting pipes fixed to the plates of the LTF. In the case of tight fitting connections or in the case of welding of the stud to the steel pipe such low stiffness of the curve segment would have been removed. All tested connections exhibited a ductile failure, with the development of two plastic hinges in the stud shank: one plastic hinge in the portion embedded in the mortar overlay and one developing along the portion driven into the steel pipes. It is worth noting that the sole stud connection at the edge of the wall (position 1' in Fig.10b) showed a different failure mechanism, characterised by the tensile failure of the masonry; interestingly, such failure occurred after the yielding of the connection.

Besides the small initial clearance recovery, pinching of the curve is also induced by the incremental damage of the mortar layer due to repeated load reversal. Collapse occurred with thinner cracks opening radially around the stud head in the mortar overlay (Fig. 11b), and the envisioned two plastic hinge mechanism of the connector (Fig. 11c). Results obtained from the four tests carried out on Specimen A are summarised in the Appendix. For the tested connections, the average yielding displacement and load are equal to $s_{y,av}$=1.67mm and $V_{y,av}$= 29.5 kN, respectively. The average capacity is $V_{max,av}$ =34.7 kN. The average shear load at 1 mm slip after clearance recovery is $V_{1,av}$ = 28.8 kN.

The experimental average value of the yielding load of the stud connection matches well with the theoretical prediction obtained from Eq. 1 and 2. By setting d=20 mm, χ=2, a=27.5 mm, f_{mh} = 44 MPa, f_y = 355 MPa in Eq. 2, the effective length can be calculated: l_{ef} = 26 mm=1.32 d. Coherently with the theoretical model assumptions, the effective length is smaller than the overlay thickness t_m and the plastic hinge is expected to develop within the overlay thickness. Finally, the theoretical yielding shear action is obtained by introducing l_{ef} in Eq. 1 and it is equal to V_{th}=23.2 kN.

a)

b)

c)
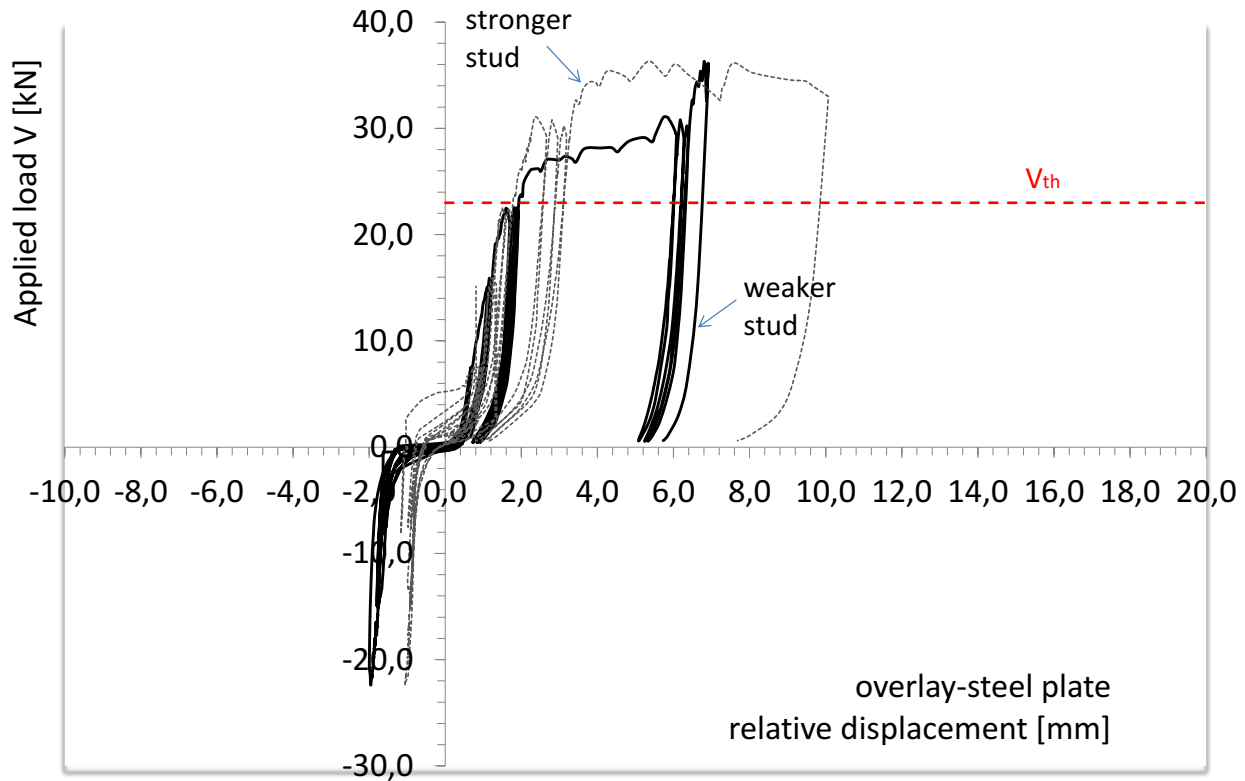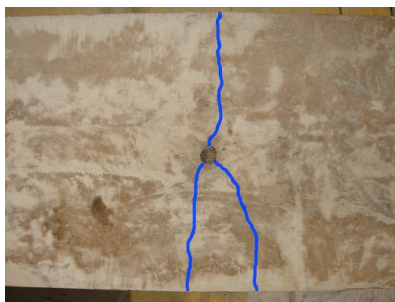
d)

Figure 11. Specimen A featuring a high strength mortar overlay: a) typical load-displacement curve obtained from laboratory cyclic tests for the weaker (a) and stronger (a') stud connection (see the Appendix). The connection yielded at a shear load of 38 kN. b) At failure, cracks developed radially from the stud to the mortar overlay edges and c) collapse was reached with two plastic hinges developing in the stud shank in the portion embedded in the steel plate and in the mortar overlay. d) No crack pattern developed in the masonry.

Further laboratory tests

To better investigate the role of the lime mortar overlay on the strength of the stud connection, further experimental tests were carried out on studs embedded in a masonry sample lacking the overlay (Specimen B), and in a specimen strengthened with an average quality lime mortar overlay (Specimen C).

The typical load-displacement curve obtained from the tests on the stud connections in Specimen B, lacking the lime mortar overlay, is plotted in Fig. 12c. As expected, no remarkable shear capacity is observed if no strengthening of the top of the masonry wall is considered. The curve shows a very low connection capacity which is usually associated with the early failure of the connection due to either: a) overcoming sliding shear resistance along the masonry bed joints, caused by the reduced friction resistance in the absence of vertical loads; b) crushing of the bricks induced by the high stress concentration; or c) diagonal shear failure of the corner portion of the masonry wall. Average connection capacity is approximately equal to 4.5 kN, and is related to a relative displacement between the steel plate and the overlay of about 3 mm. Collapse is brittle, with crushing of the upper layer of bricks (Fig. 11b), which are unable to withstand the high stresses transferred by the stud connection.
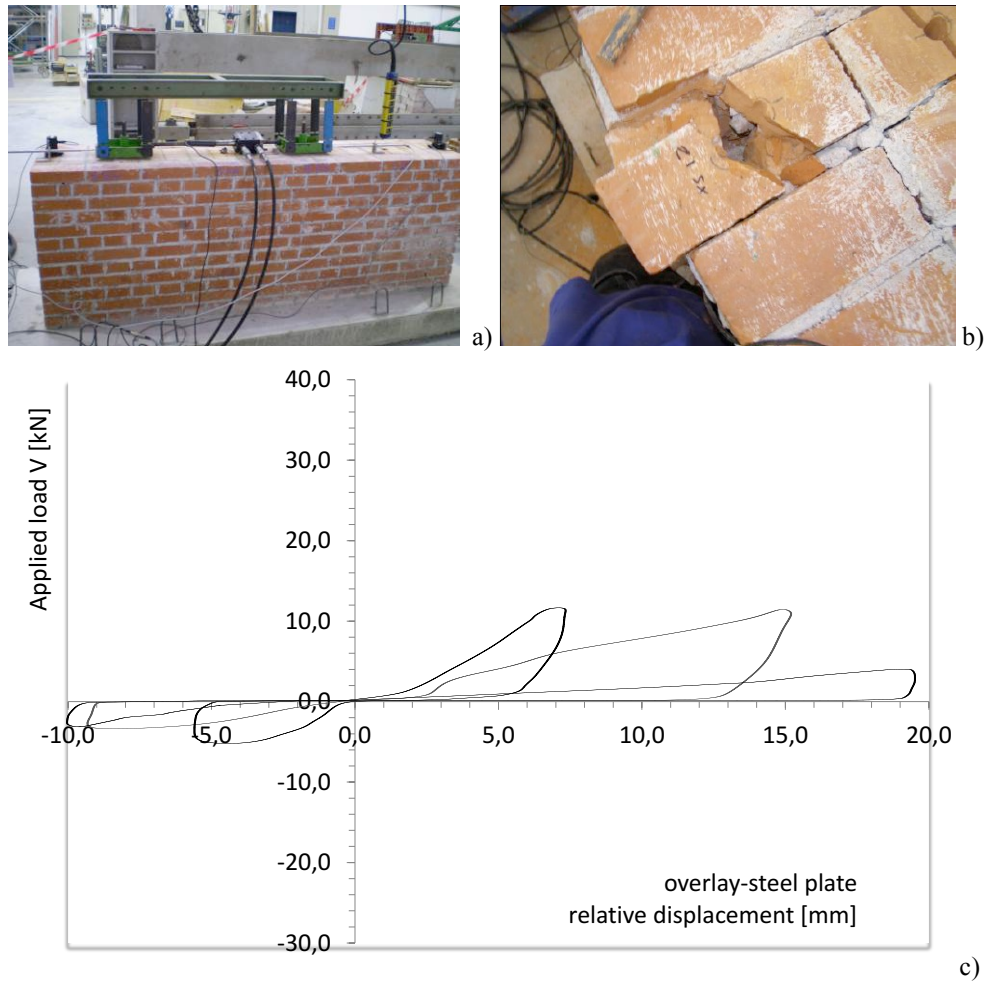
Figure 12. Specimen B. Details of the specimen a) before and b) after the laboratory tests. c) Envelope load-displacement curves obtained in three different cyclic tests; studs with 20 mm diameter and 400 mm embedment length collapsed for shear loads ranging between of 5÷10 kN with sliding shear failure of the upper layers of bricks.

In Specimen C the mortar overlay was made of lime mortar with regular characteristics; the design mix comprises 8% natural lime mortar NHL 3.5, 5% putty lime, 36% 1.5mm gravel, 36% 3mm gravel and 15% water. The average compressive strength of mortar M1 is 1MPa after 28 days curing and 2 MPa after 120 days (average of 6 samples). As in Specimen A, the overlay was strengthened with glass fibre mesh, thereby improving the bearing strength of the lime mortar up to 6.5 MPa.

Studs tested on Specimen C, introducing a poor quality mortar overlay, outperformed the connections of Specimen B; however the connection failure mode was often followed or even anticipated by the brittle failure mechanisms of the masonry, as in Specimen B, regardless of the position of the stud along the specimen (intermediate or edge position). When the failure was ductile, it was often associated with the onset of one plastic hinge developing in the stud segment

inserted in the LTF steel pipes either with or without a second plastic hinge developing along the portion embedded in the masonry.

Figure 13 shows a typical load-displacement curve obtained from the tests on the stud connections in Specimen C. The initial gap of the curve follows the slackness recovery, whereas the remarkable pinching of the curve is increased by the progressive plasticisation of the mortar overlay. The substantial reduction of the net cyclic stiffness for different cycles at equal load provides evidence of the incremental damage of the mortar layer due to increasing load reversal. Results obtained in the 4 tests carried out on Specimen C are summarised in the Appendix.

For the weaker connection, the average shear load at 1 mm net of relative slip is equal to $V_{1,av}$=8.6 kN, whereas the yielding displacement and load are equal to $d_{y,av}$=3.2 mm and $V_{y,av}$ = 16.8 kN, respectively. The average capacity is $V_{max,av}$=17.9 kN. The connection illustrated in Figure 13 shows an example of ductile failure, with cracks spreading radially across the mortar overlay and two plastic hinges in the stud, one within the steel plate and one within the masonry; the development of plastic hinges in the stud was followed by the masonry failing in sliding shear.

It is worth noting that the aforementioned analytical model cannot be applied to predict the capacity of both Specimen B and C; indeed, the dowel shank cannot be assumed as embedded into an homogenous material because the top of the masonry specimen is either un-strengthened or poorly reinforced.

By comparing Fig. 11a, 12a and 13a, it can be observed that the stud connections tested on Specimen A, featuring a high-performing mortar overlay, remarkably outperformed the stud connections of both Specimen B and C. Pinching of the curve is still observed in Figure 11a but its amplitude is almost halved with respect to the tested connections of Specimens C. The same observation applies to the reduction of the net cyclic stiffness, which confirms a reduction in the incremental damage of the mortar layer for increasing load reversal with respect to Specimens C.
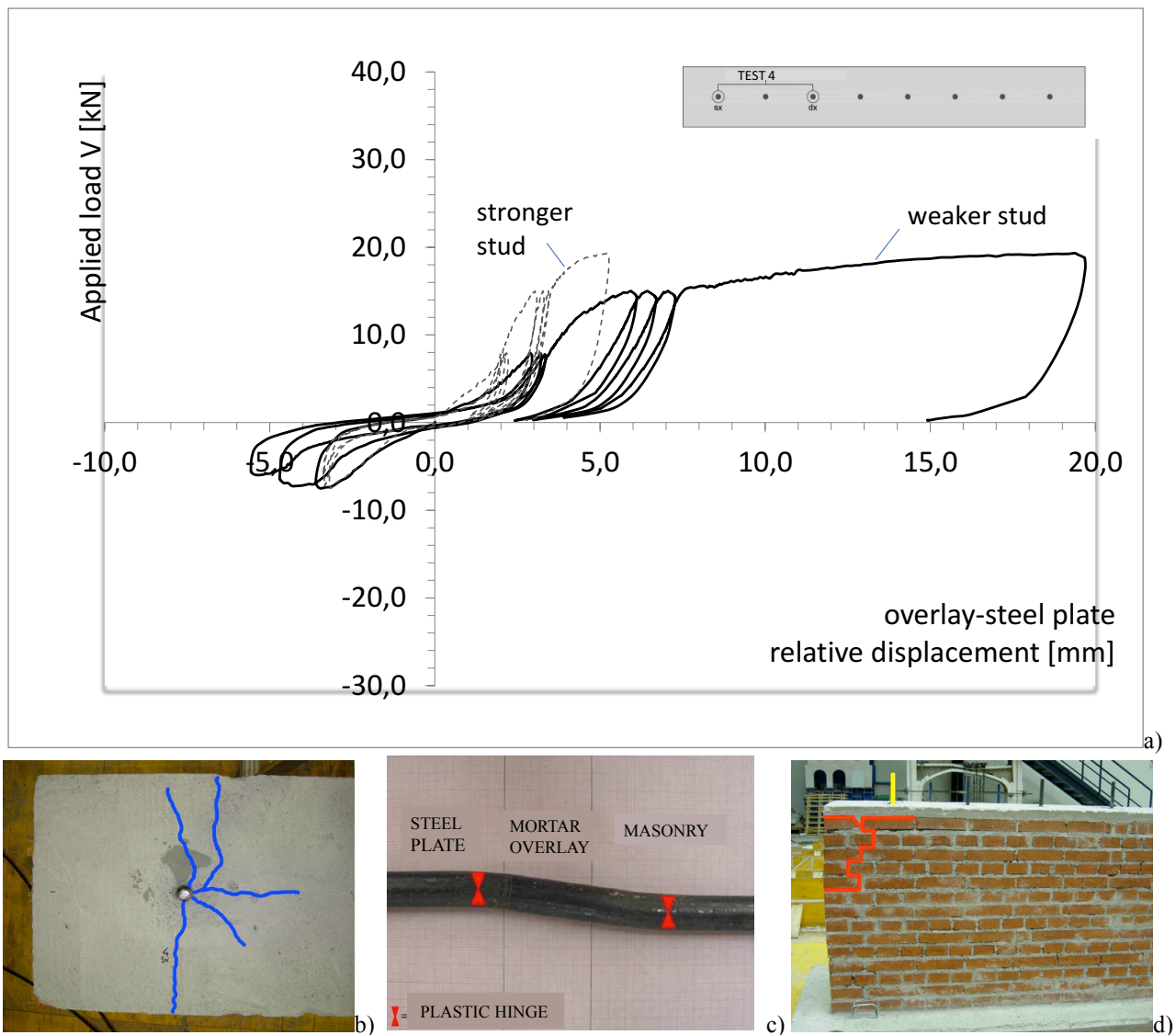
Figure 13. Specimen C with low strength mortar overlay: a) typical load-displacement curve obtained in laboratory cyclic tests (Specimen C, Test 4, see the Appendix). The stud connection yielded at a shear load of 15 kN. b) At failure, cracks developed radially from the stud to the mortar overlay edges and c) collapse was reached with two plastic hinges developing in the stud shank in the portion embedded in the steel plate and in the masonry. d) Sliding shear failure of the upper brick layers at the masonry wall corner.

4.2 On-site experimental study

Testing frame for on-site tests

For on-site testing, the lightweight and portable apparatus shown in Figure 14 was developed. The testing frame is made of aluminium in order to enable easy transportation, and it is suitable for monotonic loading tests of pairs of studs, like the apparatus adopted for the laboratory tests. The studs (*1* in Fig. 14) are connected to the steel plates (*2*) in the same way as in real roof shell structure connections. As described in section 3, the connection between the stud and the plate can be assumed as rigid in the case of tight fitting connections, or in the case of full penetration welding

of the stud to the plate (Fig.9c). The connection is considered as pinned if hole-stud clearances are present, or considered as semi-rigid in the case of partial penetration welding (Fig.9d).

Steel plates resembling the perimeter chords of actual roof shell structures are adopted. Steel plates are placed above the roof shell plywood panels, with thickness a, which in turn lies above the lime mortar layer overlaying the top of the masonry wall. The shear action F to be applied to the studs is developed by means of a torque wrench (*3* in Fig.14) and transferred to the plates by means of the vertical elements (*4* in Fig.14) connected by the transverse plate (*4'* in Fig.14). Spherical washers (*3'* in Fig.14) are introduced to enable rotation of the vertical elements (*4* in Fig.14). The transverse plate (*4'* in Fig.14) has a low rotational stiffness and can therefore be considered as a truss connecting the vertical elements (*4* in Fig.14).

Rotation of the steel plates (*2* in Fig.14), which is caused by the small eccentricity e between the shear action F and the sliding plane, is prevented by the pressure exerted by the plate onto the sliding surface (Fig.14 b); such pressure results in an additional friction resistance contribution ΔF, which may distort the experimental evaluation of the stud shear capacity and must therefore be deducted from the experimental results. It is worth noting that in the actual roof shell structure, the perimeter chord is continuous and the connection rotation is negligible; therefore the subsequent friction load ΔF is also negligible. In the on-site tests, the friction load ΔF can be evaluated by enforcing balance to rotation:

$$\Delta F = F \frac{e}{\Delta l} \mu \qquad\qquad 3)$$

where Δl is the distance between the stud and the edge of plate (*2*), μ is the wood-to-steel friction coefficient, ranging between $\mu = 0.2 \div 0.3$; the eccentricity e is $e = t_s + a$, where t_s is the steel plate thickness and a is the wood panel thickness. As an additional precaution, steel plates (*2* in Fig.14) are smoothened along the edges (*2'* in Fig.14) to avoid possible interlocking in the top course of the wall. As for the instrumental setup, mechanical displacement transducers (*5* in Fig.14) record the relative displacements between the plates (*2* in Fig.14) and the masonry wall below.

Results from on-site tests

Experimental tests were carried out in several construction sites to assess the feasibility of the envisioned strengthening intervention of introducing roof shell structures, requiring efficient connections to the top of the perimeter masonry walls. Experimental tests also enabled estimation of the reference design loads of the connection, or validation of the theoretical predictions of the connection capacity obtained with the analytical formulation, when applicable.

As an example, Figure 15 shows the results obtained from the shear tests carried out on the connections securing the roof shell structure to the masonry walls in the "Madonna della Rocca" Church, a sanctuary located in Sabbio Chiese (Brescia, Italy) which was significantly damaged by the Salò earthquake in 2004. The top of the masonry walls are made of rubble stone masonry of good quality. The quality of the masonry was judged based on the procedure proposed by Borri et al. (2015). The top of the perimeter masonry walls is strengthened with a high-performance premixed lime mortar overlay of 50 mm. The mechanical properties of the premixed improved lime mortar are the same as those used in Specimen A. 20mm S355 studs were driven into 400 mm depth holes, vertically drilled in the masonry wall with a core drill. The stud heads were spot-welded to the steel plates of the testing apparatus.
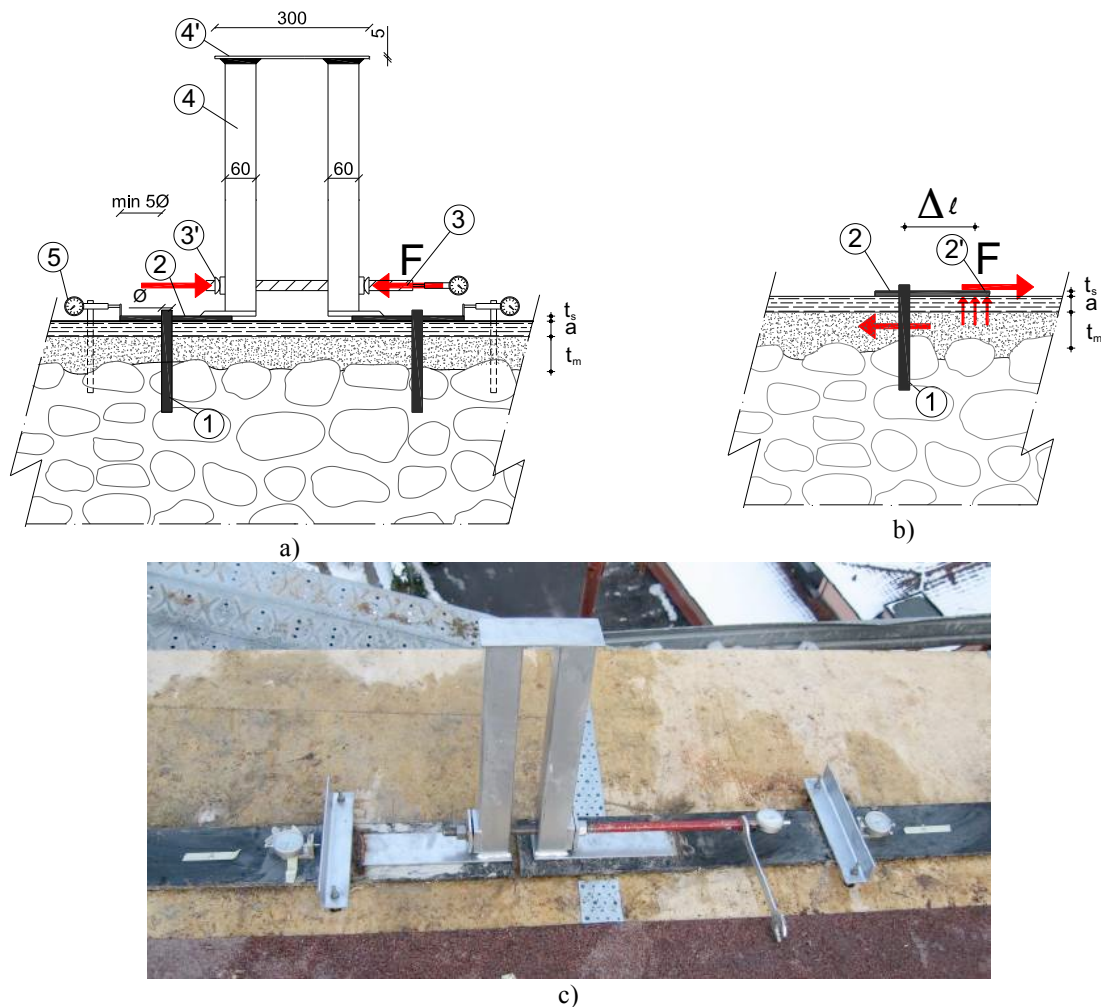

a)

b)

c)

Figure 14. a) Schematic view of the test set up; b) small eccentricity of the shear action F and the sliding plate, resulting in a pressure exerted by the plate onto the sliding surface, and therefore in an additional friction resistance contribution ΔF, to be deducted from the experimental results; c) view of the aluminium testing frame for on site tests.

23

The load–displacement curves of monotonic shear tests are shown in Figure 15b. Thanks to the spot-welding of the stud heads no initial gap in the curve is observed. For the weaker connection, the shear load at 1 mm relative slip is equal to $V_1 = 10$kN, whereas the yielding displacement and load are equal to $d_y \cong 5.6$ mm and $V_y \cong 24$kN, respectively. Collapse occurred with thinner cracks opening radially around the stud head in the mortar overlay, and following the onset of the envisioned 2 plastic-hinge mechanism of the connector.

The experimental yielding strength compares well with the theoretical prediction obtained from Eq. 1, which yields V_{th}=23.5 kN (with d=20 mm, χ= 2, a=27 mm, f_{mh} = 44 MPa, f_y = 355 MPa yielding an effective length of about: l_{ef}= 27 mm = 1.33 d). The spacing of the connection was selected to provide a capacity equal to twice the design load in order to obtain an over-resistant system.
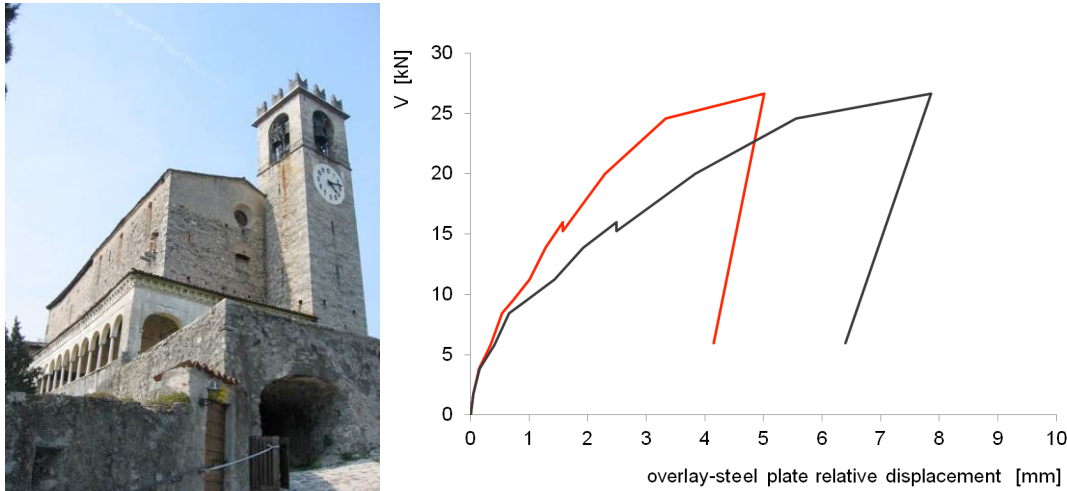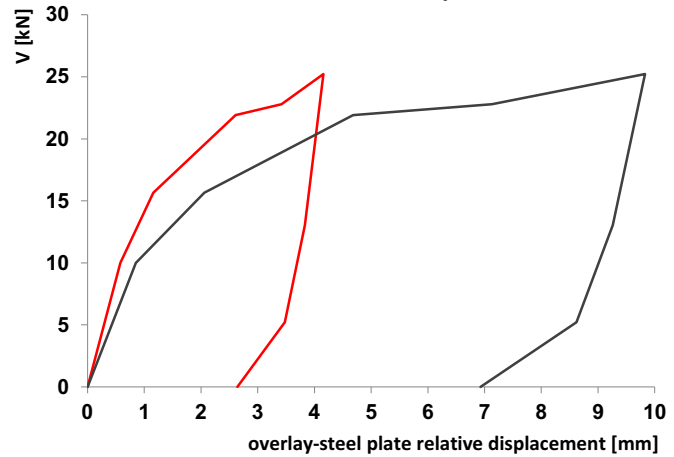

Figure 15. Example of in-situ tests. Madonna della Rocca, Sabbio Chiese, Italy.

(a) S. Maria Assunta, Bione, Italy
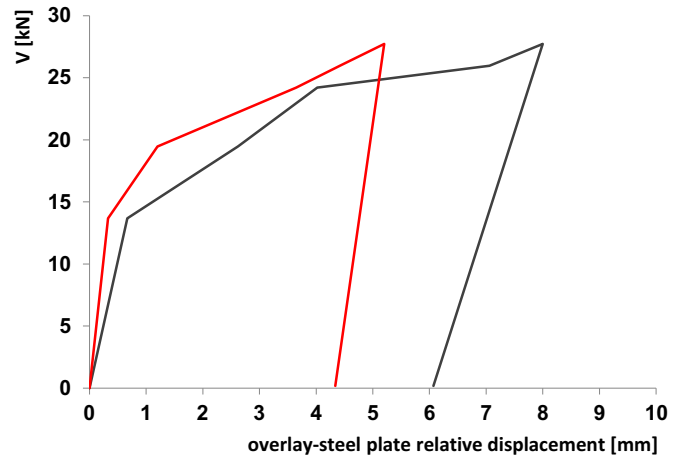
24

(b) SS. Trinità, Roè Volciano, Italy

Figure 16: In-situ tests results obtained in two Churches in northern Italy.

Other examples of in-situ test results carried out on two churches located in northern Italy are shown in Figure 16. Both churches are made of rubble stone masonry of good quality (Borri et al. 2015). The materials used for the thin lime mortar overlay and for the roof shell structure are the same as those adopted in the Madonna della Rocca Church. The experimental yielding strength V_y compares well with its theoretical prediction in these cases as well, confirming the reliability of the theoretical model.

When an improved lime mortar overlay is introduced on the top of the masonry walls the capacity of the connection is no longer governed by the heterogeneous properties of the masonry, but rather by the properties of the thin, high-performance strengthened lime mortar slab. This is evidenced by the quite similar connection capacity measured through in-field tests in the different construction sites (Fig. 15-16, further evidence can be found in the examples presented in Marini et al. 2016), featuring different masonry characteristics, but where the same geometrical and mechanical properties of the high-performance overlay and the steel dowel connection were adopted.

Besides the limited number of presented applications, it is worth noting that a larger number of tests would not provide any further information or relevant reference statistics. Indeed, when the proposed improved lime mortar overlay is missing, the capacity of the connection would entirely depend on the heterogeneous properties of the masonry, therefore no reference value of the connection capacity could be addressed, but rather specific in-field assessment would be required. On the other hand, when such overlay is applied to the top of the masonry wall, the stud capacity is dependent on the properties of the slab, and is not significantly affected by the properties of the masonry. Finally, it is worth noting that, regardless the applicability and reliability of the analytical formulation, in-field tests are always mandatory in order to assess the correct execution of the

25

connections and the effectiveness of the pre-consolidation of the top of the masonry wall, particularly concerning the actual attainment of high performances of the thin lime mortar slab. Nonetheless, accuracy of the construction steps must be verified with in-situ tests.

5. CONCLUDING REMARKS

Seismic vulnerability of historical masonry structures is often governed by the onset of local mechanisms such as the overturning of the perimeter walls. In churches, the failure of the nave vaults could be triggered by the unconstrained rocking of the transverse arches. Traditional seismic retrofit of such buildings consists in the adoption of either perimeter ties, or floor and roof diaphragms aimed at inhibiting local mechanisms and engaging a box-like structural behaviour of the whole building. Although minimally impairing interventions such as the perimeter ties are usually preferred, there are situations in which "light interventions" are unviable, as in the case of poor quality masonry, slender walls and discontinuity of the perimeter walls. In all these cases diaphragms are usually preferred.

The correct detailing of the diaphragm is fundamental for the effectiveness of the retrofit. The connection is a particularly critical component of the envisioned box-like structure, given that it must enable substantial shear transfer between the roof-diaphragm and the perimeter masonry walls at the eave level, where small vertical confining actions may jeopardise the shear resistance of the masonry, which entirely relies on friction.

In this paper, the use of roof diaphragms was investigated; focus was placed on the design and structural performance assessment of the dowel connections to the perimeter walls. Dowels are designed to enable the transfer of shear flow from the out-of-plane loaded masonry walls to the roof-diaphragm, and from the roof-diaphragm to the seismic resistant walls. Further stud connections may be needed to secure other structural elements, such as the transverse arches in churches, to the box structure.

In the paper, specific structural detailing for the pre-pre-consolidation of the top portion of the masonry walls was proposed in order to improve the connection shear resistance. Pre-consolidation, obtained by introducing a thin lime mortar overlay strengthened by glass fibre mesh, was shown to effectively increase the capacity of the connection by improving its structural behaviour. It was also observed that in the case of poor quality masonry, such as three-leaf masonry walls lacking perpend stones, further substantial preliminary retrofit of the masonry is mandatory in order to enforce a monolithic behaviour of the wall, prior to the introduction of the high strength overlay.

In general, the theoretical behaviour of the stud connection can hardly be modelled because of the substantial dis-homogeneity of the masonry at local level, particularly in the case of historic masonry buildings. Analytical formulations for roof-to-wall dowel connections are reliable only if the dowel can be assumed as completely embedded into a homogeneous material; such a condition is associated with good quality masonry and with pre-consolidated masonry walls featuring a mortar overlay thicker than the effective length of the dowel (equal to 1.5 times the diameter of the stud). In the latter hypothesis, an analytical model was presented for estimation of the capacity of the dowel connection suitable for its preliminary design.

Given the above, experimental approaches are necessary to assess the actual stud capacity on-site. A new experimental test was conceived. Special testing frames, to be used for laboratory and in-situ tests, were specifically designed to mimic the actual load and restraint conditions of the connection in a real application. Cyclic and monotonic load vs relative displacement curves were obtained from laboratory and in-situ tests, respectively, and provided evidence of the envisioned structural behaviour of the connection. When the capacity of the connection is improved through the mortar overlay, the failure of the connection was reached with the development of two plastic hinges in the bolt shank. Finally, it is worth noting that, regardless of whether the analytical formulation can be applied, in-field tests are always mandatory in order to assess the correct execution of the connections and the effectiveness of the pre-consolidation of the top of the masonry wall, particularly concerning the actual attainment of high performances of the thin lime mortar overlay and the viability of the envisioned strengthening solution.

6. ACKNOWLEDGEMENTS

7. REFERENCES

1) American Concrete Institute Committee 318 (ACI), 2008. Building Code. Requirements for Structural Concrete (ACI 318-08) and Commentary (ACI 318R-08), American Concrete Institute, Farmington Hills, Michigan.
2) ACI 530/530.1-13: Building Code Requirements and Specification for Masonry Structures and Companion Commentaries.

3) Ahmadi, B. H., and Saka, M. P. 1993. Behavior of composite timber-concrete floors. J. Struct. Eng., 119(10), 3111–3130.

4) Auclair, S.C., Sorelli, L., Salenikovich, A. 2016. Simplified nonlinear model for timber-concrete composite beams. International Journal of Mechanical Sciences. Volume 117, October 2016, pp. 30–42

5) Biolzi, L. & Giuriani, E. 1990. Bearing capacity of a bar under transversal loads. Materials and Structures (1990) 23: 449. doi:10.1007/BF02472028

6) Borri A., Corradi M., Castori G., De Maria A. 2015. A method for the analysis and classification of historic masonry Bulletin of Earthquake Engineering 13(9). DOI10.1007/s10518-015-9731-4

7) Carbonara, G. 2003. Trattato di restauro architettonico. UTET Ed.

8) Cominelli, S., Giuriani, E., Marini, A. 2016. Mechanisms governing the compressive strength of unconfined and confined rubble stone masonry. *Material and Structures*. Vol. 50(1), February 2017. doi: 10.1617/s11527-016-0905-6.

9) D'Ayala, D., and Speranza, E. 2002. An integrated procedure for the assessment of seismic vulnerability of historic buildings [CD-ROM]. Proceedings of the 12th European Conference on Earthquake Engineering, paper n. 561 London, England: Elsevier Science.

10) D'Ayala, D. 2014. Conservation Principles and Performance Based Strengthening of Heritage Buildings in Post-event Reconstruction. Geotechnical, Geological and Earthquake Engineering. Vol. 34, pp. 489-514.

11) Eurocode 5. 2005. Design of timber structures. European Committee for Standardization (CEN). UNI EN 1995:2005. Brussels.

12) Eurocode 8. 2004. Design of structures for earthquake resistance. European Committee for Standardization (CEN). UNI EN 1998.

13) ETAG 029, Metal injection anchors for use in masonry. 2010

14) Felicetti, R., Gattesco, N., Giuriani, E. 1997. Local phenomena around a steel dowel embedded in a stone masonry wall. Materials and Structures. Vol.30: 238. doi:10.1007/BF02486182

15) Ferrario L., Marini A., Riva P., Giuriani. E. 2009. Traditional and Innovative Techniques for the Seismic Strengthening of Barrel Vaulted Structures Subjected to Rocking of the Abutments. ATC-SEI Conference on Improving the Seismic Performance of Existing Buildings and Other Structures. San Francisco, California, December 9 -11, 2009.

16) Gattesco, N., and Del Piccolo, G. 1998. Shear transfer between concrete members and stone masonry wall through driver dowels. European Earthquake Engineering, 1.

17) Gattesco, N., and Giuriani, E. 1996. Experimental Study on Stud Shear Connectors Subjected to Cyclic Loading. Journal Constructional Steel Research, Vol. 38. No.1, pp. 1–21.

18) Gelfi, P., Giuriani, E., Marini, A. 2002. Stud shear connection design for composite concrete slab and wood beams. ASCE Journal of Structural Engineering. Vol. 128, n.12, pp 1544-1550. ISSN 0733-9445.

19) Giuriani, E. 2011. Consolidamento degli edifici storici. Trattato di restauro architettonico. Ed. UTET. Torino, ISBN 978-88-598-0763-6.

20) Giuriani, E., Gattesco, N., Del Piccolo, M. 1993. Experimental tests on the shear behavior of dowels connecting concrete slabs to stone masonry walls. Materials and Structures. Vol. 26: 293. doi:10.1007/BF02472951

21) Giuriani, E. and Grisanti, A., 1986. Behaviour of stud connectors under repeated loads. Studi e Ricerche Corso di Perfezionamento delle Costruzioni in C.A. F.lli Pesenti, Politecnico di Milano *8 271–305*.

22) Giuriani, E., Marini, A. 2008a. Experiences from the Northern Italy 2004 earthquake: vulnerability assessment and strengthening of historic churches. Invited paper. VI International Conference on Structural Analysis of Historical Constructions SAHC 2008. 2-4 July, Bath, England. pp. 13-24. Ed. Taylor and Francis, London, UK. ISBN 978-0-415-46872-5.

23) Giuriani, E., Marini, A. 2008b. Wooden roof box structure for the anti-seismic strengthening of historic buildings. *Journal of Architectural Heritage: Conservation, Analysis and Restoration*. ISSN 1558-3058 Vol.2 (3) pp. 226-246.

24) Giuriani, E., Marini, A., Porteri, C., Preti M. 2009. Seismic vulnerability of churches associated to transverse arch rocking. *International Journal of Architectural Herita*ge, 3: 1–24, 2009. Ed. Taylor & Francis Group, LLC. ISSN: 1558-3058.

25) Giuriani, E., Marini, A., Preti, M. 2016. Thin-folded shell for the renewal of existing wooden roofs. *Journal of Architectural Heritage*. Vol. 10(6), 17 August 2016, pp. 797-816. DOI: 10.1080/15583058.2015.1075626

26) Griffith M. C., Magenes G., Melis G., and Picchi L. 2003. Evaluation of out-of-plane stability of unreinforced masonry walls subjected to seismic excitation. Journal of Earthquake Engineering 7(special issue 1): 141–169.

27) Hume, I., 1991. Conservation engineering—an English Heritage view. In Proceedings of STREMA (Structural Repair and Maintenance of Historical Buildings), Seville, 1991, pp. 3–12.

28) Johnson R.P., 2008. Calibration of resistance of shear connectors in troughs of profiled sheeting Proceedings of the Institution of Civil Engineers - Structures and Buildings, Volume 161(3)

29) R.P. Johnson, D.J. Oehlers, 1996. Integrated static and fatigue design and assessment of stud shear connections in composite bridges. Struct. Engr, 74 (14), pp. 236–240

30) Lagomarsino, S., Podestà, S., Risemini, S., Curti, E., Parodi, S., 2004. Mechanical models for the seismic vulnerability assessment of churches. *In Structural analysis of historical construction (C. Modena, P. B. Lourenço, P. Roca Eds.), Proc. of IV Int. Seminar SAHC,* Padova, Italy, A.A. Balkema, London (UK), Vol 2, pp. 1091-1101.

31) Mainstone, R.J. and Menzies, J.B. 1967. Shear Connectors in Steel-Concrete Composite Beams for Bridges; Part 1, Static and Fatigue Tests on Push-out Specimens. *Concrete*, Vol. 1, No. 9, pp. 291–302.

32) Marini A., Cominelli S., Zanotti C., Giuriani E., 2018. Improved natural hydraulic lime mortar slab for compatible retrofit of wooden floors in historical buildings. Construction and Building Materials, 158, 801–813; https://doi.org/10.1016/j.conbuildmat.2017.10.010.

33) Marini, A., Giuriani, E., Lugoboni, M., Cominelli, S., Belleri, A. 2016. Le connessioni tra le coperture scatolari sismiche e le pareti perimetrali degli edifici storici. Technical Report 3/2016, Department of Civil Engineering, Architecture, Land, Environment and Mathematics of the University of Brescia. (In Italian).

34) Marini, A., Giuriani, E., 2006. Transformation of wooden roof pitches into antiseismic shear resistance diaphragms. V International Conference on Structural Analysis of Historical Constructions. November 6-8. New Delhi. MacMillan India Ltd (Ind). ISBN. 10: 1403-93156-9. pp. 445-452.

35) Menzies, J.B., 1971. CP117 and Shear connectors in Steel-Concrete Composite Beams made with Normal-density or Lightweight Concrete. Structural Engineer, Vol. 49, No. 3, pp. 137–154.

36) Modena, C., Casarin, F., DaPorto, F., Garbin, E., Mazzon, N., Munari, M., Panizza, M., Valluzzi, M.R., 2009. Structural interventions on historical masonry buildings: Review of eurocode 8 provisions in the light of the Italian Experience. Proceedings of Eurocode 8 perspectives from the Italian Standpoint workshop. In: Cosenza E (ed) 225-236, 2009 Doppiavoce, Napoli.

37) Oehlers, D.J., Johnson,R.P., 1987. The strength of stud shear connections in composite beams. Structural Engr, 65B (2) (1987), pp. 44–48

38) Pallarés, L., Hajjar, J.H., 2010. Headed steel stud anchors in composite structures, Part I: Shear. Journal of Constructional Steel Research. Volume 66, Issue 2, February 2010, pp. 198–212.

39) Piazza, M., and Turrini, G., 1983. Il recupero statico dei solai in legno. Recuperare (7): 396–407.

40) Preti M., Loda S., Bolis V., Cominelli S., Marini A. and Giuriani E., 2017. Dissipative roof diaphragm for the seismic retrofit of listed masonry churches. Journal of Earthquake Engineering. pp. 1-21. http://dx.doi.org/10.1080/13632469.2017.136022

41) Ronca, P., Gelfi, P., and Giuriani, E., 1991. The behaviour of a wood-concrete composite beam under cyclic and long term loads. Proc., Structural Repair and Maintenance of Historical Buildings II: 2nd International Conference. Stremah 91. Brebbia, C. A., Seville, Spain, Vol. 1, 263–275.

42) Shim, C.S., 2004. Experiments on limit state design of large stud shear connectors. KSCE J Civ Eng (2004) 8: 313. doi:10.1007/BF02836013

43) Stark, JWB, van Hove BWEM., 1991. Statistical analysis of push tests on stud connectors in composite steel and concrete structures. Report BI-91-163, TNO, Delft, September 1991.

44) Tomăzevič, M., 1989. Some aspects of structural strengthening of historic buildings in urban and rural nuclei against earthquakes. Euro. Earthquake Engng No. 1 (1989) 19–40.

45) Turnšek, V., Terčelj, S., Sheppard, P. and Tomaževič, M., 1978. The seismic resistance of masonry walls and buildings. In Proceedings of 6th European Conference on Earthquake Engineering, Dubrovnik, Vol. 3, pp. 255–262.

46) Xue, W., Ding, M., Wang, H., Luo, Z., 2008. Static behavior and theoretical model of stud shear connectors. Journal of Bridge Engineering. Volume 13, Issue 6, pp. 623-634

47) Zandonini, R, and Bursi, O. S., 2002. Cyclic Behavior of Headed Shear Stud Connectors. Composite Construction in Steel and Concrete IV. ASCE, Reston, Virginia, pp. 470–482.

APPENDIX - Laboratory test results on stud connections in Specimen A and C

Laboratory test results on stud connections in Specimen A and C are summarised in Table A in terms of (Fig. A):

- *Yield Load* and *net yield displacement* (V_y, s_y), excluding the initial recovery of possible clearances;
- *Nominal Shear Capacity V_{10}* defined as the shear load at 10 mm net of relative slip;
- *Maximum applied load V_{max}*;

- *Net Initial Stiffness K:* defined as the initial slope of the curve in which initial inelastic slip induced by stud-hole clearance recovery is removed. Note that it may substantially differ from the Gross Cyclic Stiffness, defined as the slope of the line connecting two subsequent load reversal points, which reduces due to incremental damage caused by the repeated sliding. The net initial stiffness corresponds to V_1 defined as the shear load at a net relative slip of 1mm, excluding the initial recovery of clearances anytime $V_1 < V_{max}$;
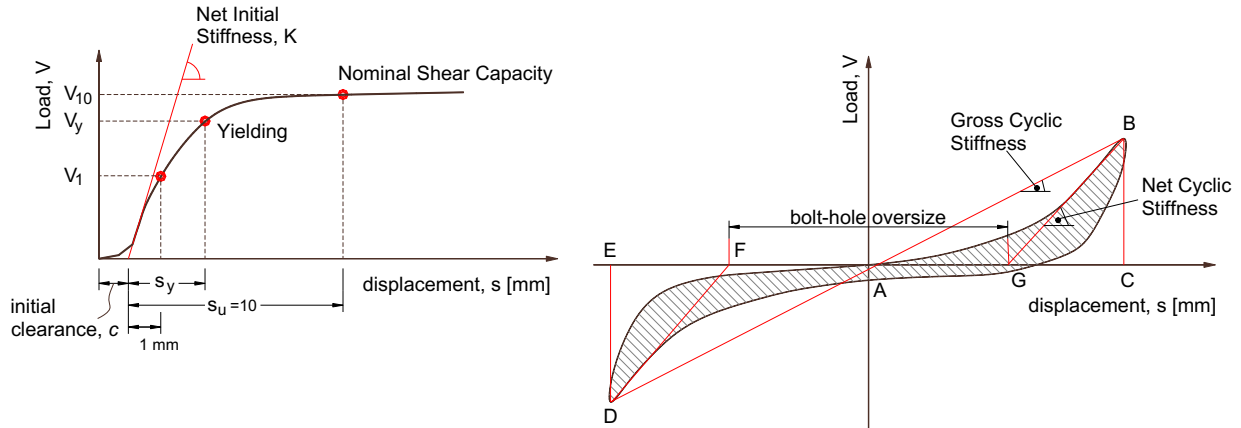

Fig. A: Main properties of the envelope curve and properties of the single load cycle.

Table A. Main results obtained from laboratory tests.

Specimen	n. test	V_y [kN]	s_y [mm]	V_{10} [kN]	V_{max} [kN]	Type of collapse	K [kN/mm] V_1 [kN]
A	1a	35	1.6	-	37.8	Ductile	30.5
A	1b	-	-	-		-	32.0
A	2a	34	1.8	-	38	Ductile	28
A	2b	35	1.7	-		-	32.0
A	3a	24	1.0	-	27	Ductile	40
A	3b	22	1.5	-		Ductile	21
A	4a	26	2	-	36	Ductile	23
A	4b	31	2.1	36		Ductile	24
	Average	*29.5*	*1.67*		*34.7*		*28.8*
C	1a	-	-	-	12.6	Brittle	4
C	1b	-	-	-		-	4.5
C	2a	18	2.8	-	22.5	Ductile	8
C	2b	17.5	3.2	-		-	7.8
C	3a	15	2.4	-	17.3	Ductile	12
C	3b	-	-	-		-	9.2
C	4a	18	2.8	-	19.3	Ductile	14
C	4b	15.5	4.9	18		-	9.8
	Average	*16.8*	*3.22*		*17.9*		*8.6*